Solar Energy
And Sustainable Development
Refereed, biannual scientific journal issued by:
The Libyan Center for Solar Energy Research and Studies

DFT Approach for Improving the Electronic and Optical Properties of $KZnF_3$ Perovskite: Impact of Copper Doping

Noureddine Elmeskini[1]*, Younes Ziat[2], Hamza Belkhanchi[3], Ayoub Koufi[4].

[1,2,3,4]Engineering and Applied Physics Team, Superior School of Technology, Sultan Moulay Slimane University, Beni Mellal, Morocco.
[1,2,3,4]The Moroccan Association of Sciences and Techniques for Sustainable Development, Beni Mellal, Morocco.

E-*mail:* [1] noureddine.el-meskini@usms.ma ,[4]ayoub.koufi@usms.ma.

SPECIAL ISSUE ON:

The 1St International Conference on Sciences and Techniques for Renewable Energy and the Environment.
(STR2E 2025)
May 6-8, 2025 at FST-Al Hoceima- Morocco.

KEYWORDS

$KZnF_3$; Wien2k code;
Absorption coefficient;
Optical conductivity.

ABSTRACT

This study investigates the structural, electronic and optical properties of cubic perovskite $KZnF_3$, in its pure state and doped with copper (Cu) at a concentration of 12.5%, using the full-potential linearized augmented plane wave (FP-LAPW) method within the framework of density functional theory (DFT) which is implemented in the Wien2k code . Density-of-state (DOS) analysis reveals that doping significantly alters electronic properties, notably through the emergence of Cu-3d impurity states near the Fermi level, resulting in a shift towards the valence band and a decrease of the band gap to 2.72 eV. Optical properties were also analyzed through dielectric functions (real and imaginary parts), absorption coefficient, optical conductivity, refractive index and reflectivity. Cu doping enhances absorption in the visible spectrum, increases electron polarization and optimizes charge carrier mobility, boosting the material's performance in optoelectronic devices. These results highlight the key role of doping in engineering perovskite properties for advanced applications, including photovoltaic technologies, optical sensors and next-generation electronic systems.

*Corresponding author.

DOI: https://doi.org/10.51646/jsesd.v14iSTR2E.798

نهج DFT لتحسين الخصائص الإلكترونية والبصرية لبيروفسكايت $KZnF_3$: تأثير التنشيط بالنحاس

نور الدين المسكيني، يونس زيات، حمزة بلخنشي، أيوب كوفي.

ملخص: تتبحث هذه الدراسة في الخواص التركيبية والإلكترونية والبصرية للبيروفسكايت المكعب $KZnF_3$ في حالته النقية والمُطعّم بالنحاس (Cu) بتركي. 5. 12 %، باستخدام طريقة الموجة المستوية المعززة الخطية كاملة الإمكانات (FP-LAPW) في إطار نظرية الكثافة الوظيفية (DFT) التي يتم تنفيذها في كود Wien2k. ويكشف تحليل كثافة الحالة (DOS) أن التطعيم يغير الخصائص الإلكترونية بشكل كبير، لا سيما من خلال ظهور حالات شوائب النحاس ثلاثية الأبعاد بالقرب من مستوى فيرمي مما يؤدي إلى تحول نحو نطاق التكافؤ وانخفاض فجوة النطاق إلى2.72 للالكترون فولت. تم تحليل الخواص البصرية أيضًا من خلال الدوال العازلة (الأجزاء الحقيقية والتخيلية)، ومعامل الامتصاص، والتوصيل البصري، ومعامل الانكسار والانعكاسية. يعزز التطعيم بالنحاس الامتصاص في الطيف المرئي، ويزيد من استقطاب الإلكترون ويحسّن من حركة ناقل الشحنة، مما يعزز أداء المادة في الأجهزة الإلكترونية الضوئية. وتسلط هذه النتائج الضوء على الدور الرئيسي للتطعيم في هندسة خصائص البيروفسكايت للتطبيقات المتقدمة، بما في ذلك التقنيات الكهروضوئية وأجهزة الاستشعار البصرية والأنظمة الإلكترونية من الجيل التالي.

الكلمات المفتاحية: $KZnF_3$؛Wien2k؛معامل الامتصاص؛الموصلية الضوئية.

1. INTRODUCTION

The transition to renewable energy solutions has become a strategic priority worldwide due to growing environmental and economic challenges. Renewable energies, such as photovoltaics (PV), wind power and batteries, offer promising opportunities to meet ever-increasing energy demand, while minimizing environmental impacts [1, 2, 3, 4]. These technologies help reduce dependence on fossil fuels and promote sustainable development thanks to their economic, social, and ecological benefits. The identification and development of renewable, sustainable and economically competitive energy sources thus remain crucial to meeting the world's energy challenges. Among these solutions, solar energy stands out for its abundance, renewable nature and low environmental impact. Its conversion into chemical energy through processes such as artificial photosynthesis represents an innovative and indispensable approach to tackling the current energy and climate crises [5, 6, 7]. Inspired by natural mechanisms, this technology opens the way to revolutionary advances capable of transforming the world's energy system over the long term.

Indeed, these technological advances open up unprecedented prospects for transforming the global energy landscape and responding effectively to the current energy and climate crises. Among the materials emerging in this context, the ABX_3 family of cubic perovskites with a crystalline structure, and in particular the ABF3 fluorinated perovskite, stand out for their unique properties and exceptional potential for energy applications. These applications include fuel cells [8], photovoltaic systems [9], coating materials [10, 11, 12], spintronic applications [13], thermal [14], and renewable energy generation [15]. Several elements are used as A and B cations to arrange the atomic structure of fluoroperovskite ABF_3 compounds, with fluorine acting as the anion [16, 17]. Fluoroperovskite, a member of the large perovskite family, has drawn attention due to its distinct physical properties, which include high electron mobility [18], dielectric property [19, 20], magnetism [21], UV transparency, and piezoelectricity. Fluoroperovskite solids have attracted much interest in the semiconductor and lens industries [22, 23]. The absence of birefringence in the cubic perovskite materials makes them preferable candidates for lenses. The huge energy band gap that these compounds display is a noteworthy feature. These materials can be used to create glass materials that effectively transmit ultraviolet (UV) and vacuum ultraviolet (VUV) wavelengths due to their narrow absorption edges [24]. In their ideal configuration, the B

atoms occupy the centers of the octahedra formed by the X anions. These octahedra are organized in a simple cubic structure, but this crystal lattice conceals remarkable chemical and physical properties. For example, ABF3 fluoroperovskites (with A=K and B=Zn) adopt a cubic symmetry belonging to the space group $Pm\bar{3}m$ (221), where the A and B cations occupy the vertices and center of the unit cell respectively. At the same time, the F anions are positioned at the center of the faces [25, 26, 27, 28, 29]. Cubic fluoroperovskites, are characterized by their mechanical stability, elastic anisotropy, and electrical properties. These properties make these materials particularly suitable for applications in photovoltaic devices [30, 31, 32]. In addition, F anions, due to their high electronegativity, interact efficiently with A and B metal cations, giving fluoroperovskites a unique combination of structural, electrical, and thermoelectric properties. Their mechanical and thermal properties open up promising prospects in various industrial sectors, including the automotive and electronic gadget industries [33, 34, 35, 36]. Moreover, Yb3+ doped glass ceramics with $KZnF_3$ nanocrystals were fabricated successfully [37]. This structural flexibility, combined with the possibility of stabilizing fluoroperovskites by integrating organic or inorganic transition metals, makes them exciting materials for research and advanced technological applications [38, 39, 40, 41]. DFT offers a powerful framework for exploring in detail the fundamental properties of $KZnF_3$, such as electronic structure, band gap, interband transitions, and mechanical stability [42, 43]. Doping, particularly with transition metals such as copper (Cu), is an effective strategy for improving the properties of $KZnF_3$, by modifying the electronic and optical structure. This study analyzes the structural, electrical, and optical properties of the material $KZnF_3$ doped with a precise 12.5% concentration of Cu (Copper) using simulations based on density functional theory (DFT). This choice of concentration was carefully selected to optimize the interaction of the dopants with the host structure while minimizing crystal defects that could affect the overall stability of the material. DFT provides a rigorous theoretical framework for examining doping-induced modifications to the fundamental properties of $KZnF_3$, such as lattice parameters, electron density, and band structure. In particular, the aim is to assess how each type of dopant influences the band gap, essential for applications in optoelectronic devices. In addition, this approach makes it possible to investigate changes in optical properties. This research, combining advanced simulations and predictive analyses, will contribute to a broader understanding of the fundamental mechanisms involved in doping $KZnF_3$. They will also provide avenues for designing innovative materials with tuned properties, meeting the specific needs of renewable energy technologies and next-generation optoelectronic devices.

2. PACKAGE AND CALCULATION PROCESS

This study focuses on the structural, electronic and optical properties of cubic $KZnF_3$ perovskites, both in the pure state and doped with 12.5% copper (Cu). The calculations have been carried out using the full-potential linearized augmented plane wave (FP-LAPW) method, implemented in the WIEN2k code, to solve the Kohn-Sham equation within the framework of density functional theory (DFT) [44, 45, 46]., the generalized gradient correction (GGA) was employed for the exchange and correlation approximations [47]. $KZnF_3$ perovskites adopt a cubic structure characterized by the space group $Pm\bar{3}m$, typical of perovskite-structured compounds. This structure is confirmed by precisely measured crystal parameters $a_0 = b_0 = c_0 = 4.021$ Å [48], and $\alpha=\beta=\gamma=90^\circ$, in perfect agreement with available experimental data ($a_0 = b_0 = c_0 = 4.055$ Å [49]), Figure 1. To study the effect of doping, Cu atoms were introduced at a concentration of 12.5%, replacing Zn atoms at the specific Wyckoff positions, where the K atoms occupy the cube corner positions at the 1-a Wyckoff coordinates of (0, 0, 0), the metal Zn site is located at Wyckoff site 1-b (0.5, 0.5, 0.5) in positions centered on the crystal body, while the halogen atoms (F) occupy the face-centered positions at Wyckoff site 3-c (0, 0.5, 0.5), these configurations enable us to examine

in detail the changes induced by doping on the material's electronic and optical properties. The simulation parameters have been carefully chosen to ensure convergence of the calculations. A cut-off value Rmt* Kmax = 7, where Kmax is the maximum magnitude of the K vector, and Kmax represents the smallest atomic sphere radius of the unit cell. Convergence criteria were defined to an accuracy of 10^{-5} Ry for energy and 10^{-4}e for charge. With octahedral integration, a 1000 k-point mesh was used to sample the Brillouin zone intensively, ensuring high resolution of the calculated properties. In addition, the location of the central state charge was set to a value of -6 Ry, guaranteeing precise optimization of structures and electronic properties. Optimizing the crystal lattice volume was a crucial step before examining the electrical and optical characteristics to make sure the structure under study was in its condition of least energy stability. The Birch-Murnaghan equation of state, which is incorporated into the Wien2k code, was used to perform this optimization [36]:

$$E = E_0 + \frac{B_0}{B_0'}(V - V_0) - \frac{B_0 V_0}{B_0'(1 - B_0')}\left[\left(\frac{V}{V_0}\right)^{1-B_0'} - 1\right] \qquad (1)$$

Where B is the modulus of compressibility, B' the pressure derivative, E is taken as the minimum energy which is the ground state energy corresponding to the volume V_0 of the unit cell.

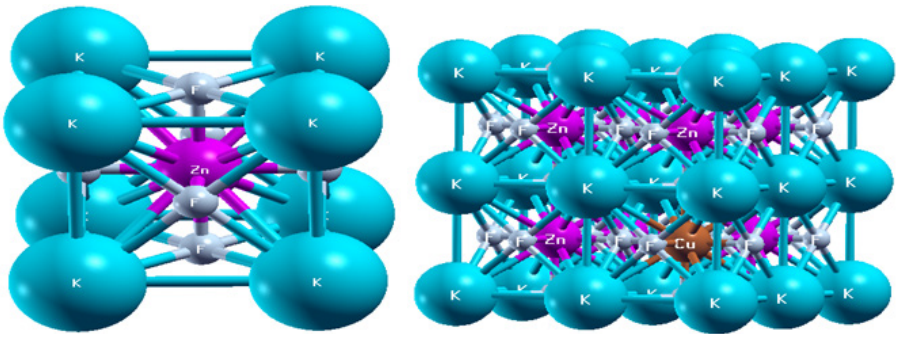

(a) (b)

Figure 1: a) The structure of the unit cell and, b) The structure of 2 × 2 × 2 Supercells of $KZnF_3$.

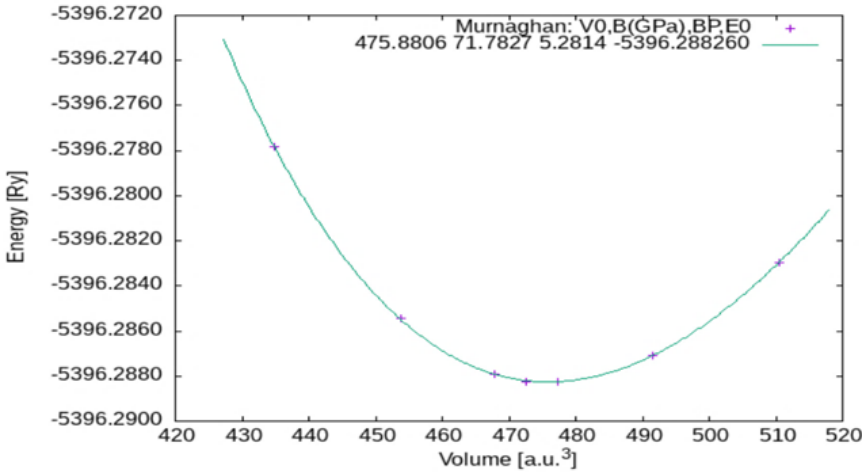

Figure 2: Variation of total energy versus volume curve of $KZnF_3$.

Figure 2 shows the volume optimization curve of total energy against the volume of $KZnF_3$-doped with 12.5% of Cu.

The optimized lattice parameters of pure $KZnF_3$ is $a_0 = b_0 = c_0 = 4.1314$ Å. The ground state derived from the optimization curve, based on the lattice parameter, is used to calculate the electronic and optical properties of the compounds self-consistently.
To model the effects of doping, a 2×2×2 supercell of pure $KZnF_3$ was constructed, in this model, some Zn sites were replaced by doping with Cu at a concentration of 12.5%. This approach enables accurate simulation of dopant-host interactions. Figure 1a illustrates the $KZnF_3$ unit cell, and Figure 1b shows the 2×2×2 supercell. This structure enables us to explore in detail the impact of doping on the crystal structure, electron density, and optical properties of the material. These results will contribute to a better understanding of the fundamental mechanisms and optimize the properties of perovskites for advanced applications in optoelectronic devices and energy technologies.

3. RESULTS AND DISCUSSION

3.1. Electronic properties

Calculations based on DFT were carried out to analyze the electronic properties of pure and doped $KZnF_3$. These calculations revealed the changes made to the electronic structure of $KZnF_3$ as a result of doping. Figure 3a and 3b show the energy band structures of the various compounds, in the energy range from -6 to 8 eV. The bandgap of the compounds are plotted along the high-symmetry path (W-L-Γ-X-W-K) in the Brillouin zone for a cubic structure, with the Fermi energy level (EF) aligned at zero. For pure $KZnF_3$ Figure 3a, an indirect band gap is observed between the L and Γ points. The bandgap width, calculated via the GGA approximation, is estimated at 3.91 eV. In doped $KZnF_3$ Figure 3b, produces subtle but significant changes in the band gap to 2.72 eV. The doped compounds exhibit similar electronic behavior, marked by electron transitions from the valence band (VB) to the conduction band (CB). Doping also induces the formation of new electronic energy levels within the band gap. These intermediate levels facilitate electronic transitions between the VB and CB, thereby improving the overall electronic properties of the material. More specifically, doped with Cu retain a direct band gap with electronic transitions in the Γ point of the Brillouin zone.

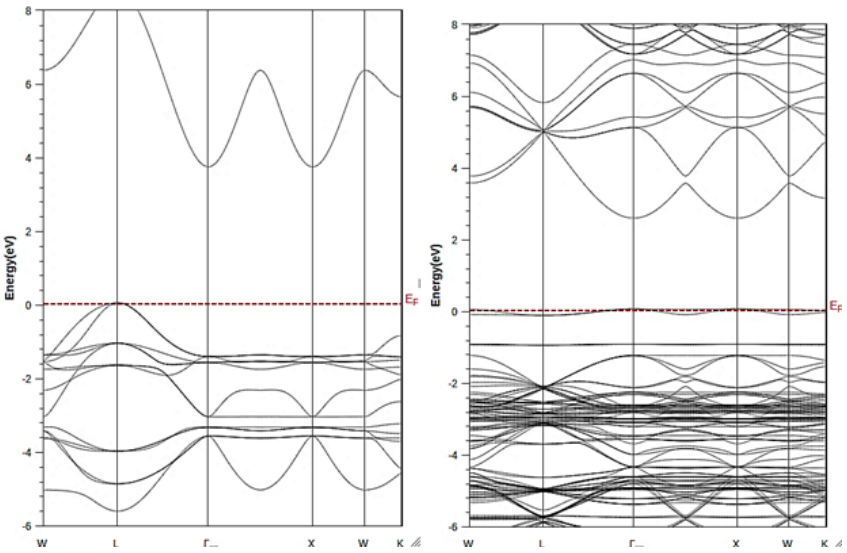

(a) (b)

Figure 3: The band structure of : a) pure $KZnF_3$; and b) doped $KZnF_3$ with Cu.

The density of states (DOS) analysis plays a crucial role in understanding the electronic properties

and chemical interactions of solid materials. In this study, the total (TDOS) and partial (PDOS) density of states of $KZnF_3$ perovskites Figure 4a and 4b, in the pure state and doped with Cu, has been examined to assess the impact of doping on their electronic properties. Calculations were performed after fully relaxing the crystal structures using the GGA potential, over an energy range from -6 eV to 7 eV, with the Fermi level fixed at 0 eV. For pure $KZnF_3$, the electronic contribution is mainly dominated by the hybridization of the K-4s and F-2p orbitals, reflecting a characteristic band structure. In doped structures, significant changes appear in the DOS, particularly at the bandgap level, with a measured reduction in band gap width to 2.72 eV. The Cu-3d doping also leads to a shift in the Fermi level towards the VB, indicating p-type semiconductor behavior. This phenomenon is attributed to an increase in hole carrier density, due to a greater concentration of F-2p states in the VB. The doped compounds also exhibit distinct electronic transitions between the VB and the CB, associated with significant hybridization between F-2p and Zn-3d electronic states in the VB, and relatively weaker hybridization in the CB.

Adding Cu atoms introduces Cu-3d impurity states that predominate in the VB, while F-2p states mainly influence the CB. This hybridization, combined with the modification of the band structure, reduces the energy gap between the VB and the CB, thus promoting a decrease in the band gap. In addition, the extra electronic states introduced by Cu near the CB create donor energy levels, facilitating electron movement.

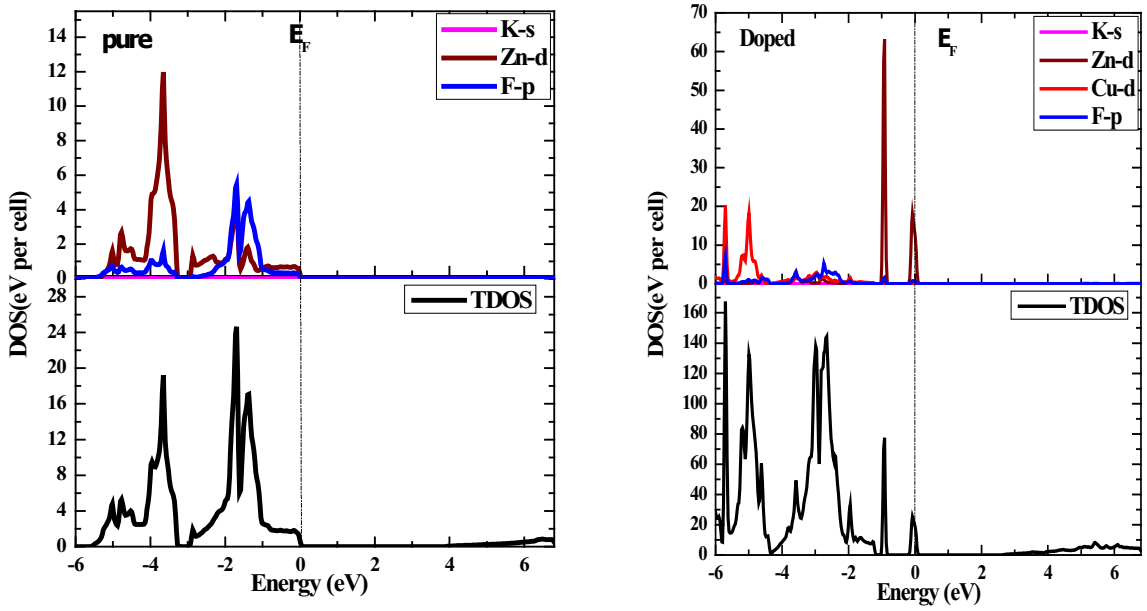

(a) (b)

Figure. 4: DOS of : a) pure; and b) doped $KZnF_3$.

This study demonstrates that Cu doping profoundly alters the electronic properties of $KZnF_3$. The decrease in the band gap, combined with the p-type behavior induced by the shift in the Fermi level, highlights the potential of this material for applications in electronic and optoelectronic devices requiring p-type conductivity. These results also open up prospects for tailoring the properties of $KZnF_3$ to the specific needs of applications ranging from semiconductors to metallic conductors, depending on the dopant used.

3.2. Optical properties

The optical properties of pure and doped $KZnF_3$ have been studied to assess the impact of dopants on its electronic structure. Various important optical parameters are presented in Figures 5 to 9.

Mathematical equations used to extract the dielectric functions (real part, $\varepsilon_1(\omega)$, and imaginary part, $\varepsilon_2(\omega)$, the absorption coefficient $\alpha(\omega)$, the optical conductivity $\sigma(\omega)$, the refractive index $n(\omega)$ and the reflectivity $R(\omega)$. The dielectric function $\varepsilon(\omega)$ was computed [50, 51]:

$$\varepsilon(\omega) = \varepsilon_1(\omega) + i\varepsilon_2(\omega) \qquad (2)$$

The dielectric function real part ($\varepsilon_1(\omega)$) is obtained through the Kramers-Kronig transformation [52, 53]:

$$\varepsilon_1(\omega) = 1 + \frac{2}{\pi} p\int \frac{\omega'\varepsilon_2(\omega')}{(\omega'^2 - \omega^2)} d\omega' \qquad (3)$$

The imaginary part ($\varepsilon_2(\omega)$) values are calculated using the following procedure [52, 54]:

$$\varepsilon_2(\omega) = \left(\frac{4\pi^2 e^2}{m^2\omega^2}\right)\sum_{i,j} \langle i|M|j\rangle^2 f_i(1-f_j)\delta(E_f - E_i - \omega) d^3k \qquad (4)$$

The element of the dipole matrix is denoted M, the electron mass is m, the elementary charge is e, and P represents the principal value of the integral in this context. The initial and final states are denoted by the indices i and j respectively. The energy of the electron in state i, with wave vector k, is denoted by E_i, and the Fermi-Dirac distribution function associated with state i is denoted by f_i.

The $\varepsilon_1(\omega)$ and $\varepsilon_2(\omega)$ components enable the determination of various optical properties, such as the absorption coefficient $\alpha(\omega)$, the optical conductivity $\sigma(\omega)$, the refractive index $n(\omega)$ and the reflectivity $R(\omega)$ using the following formula [55, 56, 57, 58]:

$$a(\omega) = \sqrt{2}\,\omega\left[\sqrt{\varepsilon_1(\omega)^2 + \varepsilon_2(\omega)^2} - \varepsilon_1(\omega)\right]^{1/2} \qquad (5)$$

$$\sigma(\omega) = \frac{\omega}{4\pi}\varepsilon_2(\omega) \qquad (6)$$

$$R(\omega) = \left|\frac{\sqrt{\epsilon(\omega)} - 1}{\sqrt{\epsilon(\omega)} + 1}\right|^2 \qquad (7)$$

$$n(\omega) = \frac{1}{\sqrt{2}}\left[\sqrt{\varepsilon_1^2(\omega) + \varepsilon_2^2(\omega)} + \varepsilon_1(\omega)\right]^{1/2} \qquad (8)$$

Figure 5a shows the variation of $\varepsilon_1(\omega)$ for pure and doped $KZnF_3$, in an energy range from 0 to 14 eV. This function describes the material's response to an electric field, in particular its ability to polarize and store electrical energy. The static dielectric constant $\varepsilon_1(0)$, which reflects polarization at low frequencies, shows a significant increase after doping. For pure $KZnF_3$, $\varepsilon_1(0)$ is 1.67, and when doped at a concentration of x = 12.5%, the values of $\varepsilon_1(0)$ increases to 6.73. This trend indicates that the introduction of dopants enhances the material's polarizability. The observed increase in $\varepsilon_1(0)$ can be attributed to the dopants' ability to induce additional dipoles, alter both ionic and electronic polarizability, and modify the local electronic structure, thereby amplifying the dielectric response of the material [59]. Figure 5b shows the $\varepsilon_2(\omega)$ for pure and doped $KZnF_3$, in an energy range from 0 to 14 eV. This parameter plays a key role in understanding the electronic absorption processes of materials. The analysis of the optical spectrum reveals several distinct peaks, resulting from inter-band transitions between the VB and CB. For pure $KZnF_3$, the spectrum reaches a notable energy peak at 5.45 eV in the ultraviolet, corresponding to electronic transitions involving K-4s, F-2p and Zn-3d orbitals in the VB, and F-2p orbitals in the CB. An increase in $\varepsilon_2(\omega)$ is observed with photon energy, peaking around 13 eV. After

Cu doping, the peaks in the spectrum undergo an energy shift to lower values, accompanied by changes in their intensity and position, including the appearance of peaks at 2 eV, associated with transitions characteristic of Cu-doped $KZnF_3$. Also, a maximum peak is observed at 0 eV, where this one is 6.5 eV. When comparing Figure 5b with Figure 4a, this value is due to the shifting of the Zn-3d state to 0 eV, where the system is being doped.

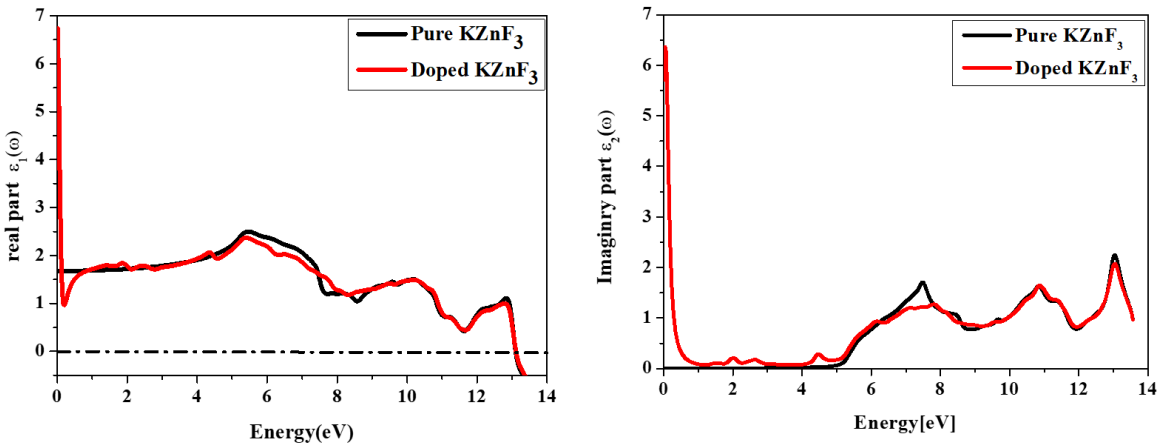

a) b)

Figure 5: Dielectric function of pure and doped $KZnF_3$: (a) Real part; and (b) Imaginary part.

Figure 6 illustrates σ(ω) for pure and doped $KZnF_3$ over an energy range of 0 to 14 eV, which represents the material's ability to transport electrons in response to an applied electromagnetic field [60]. Transparency in the 0–4.1 eV region is indicated by the absence of optical conductivity in pure $KZnF_3$, which can be attributed to the absence of light-absorbing electronic transitions.

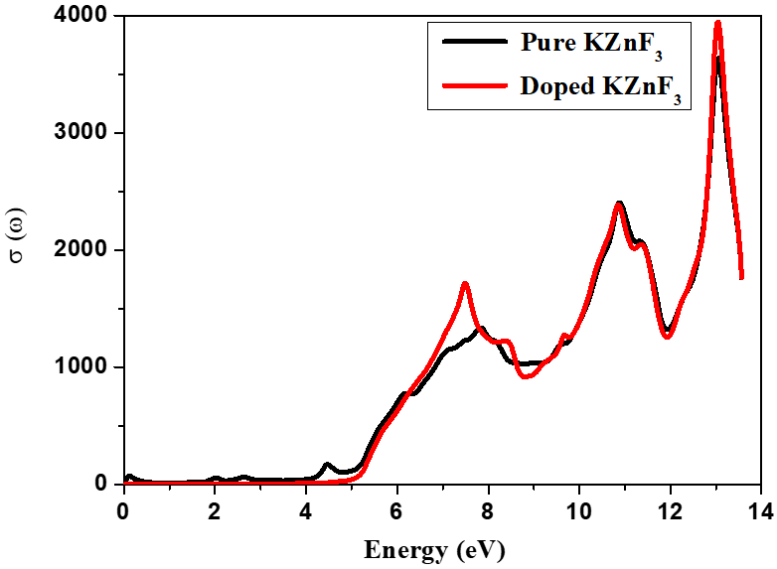

Figure 6: Optical conductivity as a function of energy of pure and doped $KZnF_3$.

Additionally, the optical conductivity of the pure $KZnF_3$ compound has a noteworthy value, increasing gradually from 4.9 eV to a maximum of roughly 13.02 eV. The conductivity maximum, as demonstrated by the previously mentioned peak, is 3614.18 $\Omega^{-1}.cm^{-1}$. The doped compound's maximum σ(ω) value is roughly 3930.88 $\Omega^{-1}.cm^{-1}$. The results show that doping changes the compound's electronic structure, which raises its reactivity at particular photon energy. Material qualities are tailored for certain applications, such as optoelectronics, even if doping reduces

maximum optical conductivity.

Figure 7 illustrates the absorption coefficient α(ω) of pure and Cu-doped KZnF3 in the energy range from 0 to 14 eV. Pure KZnF3 shows no optical absorption in the 0 to 4.5 eV range, but begins to absorb the light between 4.5 and 13.5 eV, with increasing intensity as a function of photon energy, and when doped with Cu, absorption peaks appear at 4.2 eV. This doping considerably enhances absorption properties in the visible, with coefficients reaching values as high as 10^4 cm^{-1}, and broadens absorption capacity, 12.5% Cu doping further optimizes these properties, demonstrating the material's potential for applications in photovoltaic cells and optoelectronic devices. The results indicate that the doping introduces additional electronic states favoring interband transitions, making the material capable of absorbing a greater proportion of the solar spectrum. This significant enhancement of absorption capabilities in the visible and ultraviolet range also suggests promising applications for photochemical reactions activated by visible light, reinforcing the interest of Cu-doped KZnF3 as a versatile material for advanced energy and optical technologies.

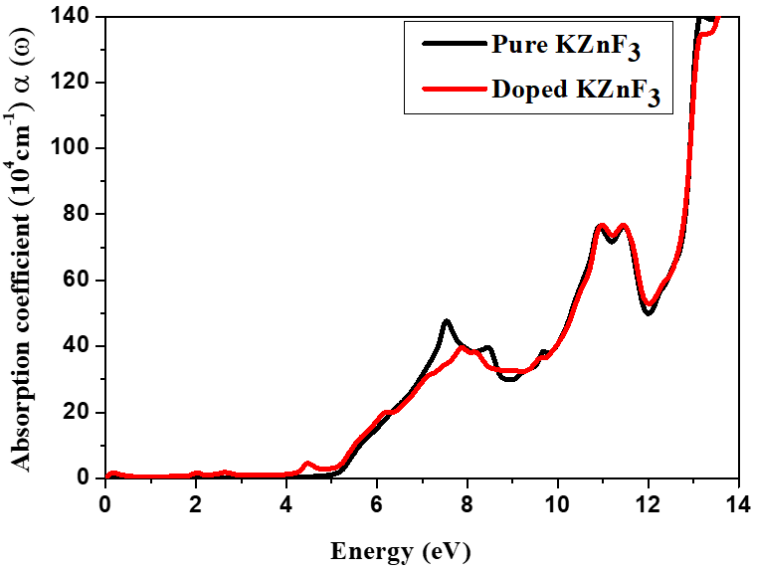

Figure 7: Absorption coefficient as a function of energy of pure and doped $KZnF_3$.

Figure 8 shows the evolution of the refractive index n(ω) of pure and Cu-doped Figure 8 shows the evolution of the refractive index n(ω) of pure and Cu-doped $KZnF_3$ over a given energy range. The results reveal that the static refractive index n(0) of $KZnF_3$, initially is of 1.25 in the pure state, increases significantly to reach a value of 2.78 after Cu doping. This reflects an enhanced interaction with light, indicating a notable improvement in the material's optical properties. Pure $KZnF_3$ exhibits its maximum refractive index at 5.9 eV, while Cu doping shifts these peaks towards 0.4 eV. By modifying the interaction between electronic bands, Cu doping transforms the optical properties of $KZnF_3$, this enhancement gives doped $KZnF_3$ greater potential for advanced optoelectronic applications. over a given energy range. The results reveal that the static refractive index n(0) of Figure 8 shows the evolution of the refractive index n(ω) of pure and Cu-doped $KZnF_3$ over a given energy range. The results reveal that the static refractive index n(0) of $KZnF_3$, initially is of 1.25 in the pure state, increases significantly to reach a value of 2.78 after Cu doping. This reflects an enhanced interaction with light, indicating a notable improvement in the material's optical properties. Pure $KZnF_3$ exhibits its maximum refractive index at 5.9 eV, while Cu doping shifts these peaks towards 0.4 eV. By modifying the interaction between electronic bands, Cu doping transforms the optical properties of $KZnF_3$, this enhancement gives doped $KZnF_3$ greater potential for advanced optoelectronic applications., initially is of 1.25 in the pure

state, increases significantly to reach a value of 2.78 after Cu doping. This reflects an enhanced interaction with light, indicating a notable improvement in the material's optical properties. Pure $KZnF_3$ exhibits its maximum refractive index at 5.9 eV, while Cu doping shifts these peaks towards 0.4 eV. By modifying the interaction between electronic bands, Cu doping transforms the optical properties of $KZnF_3$, this enhancement gives doped $KZnF_3$ greater potential for advanced optoelectronic applications.

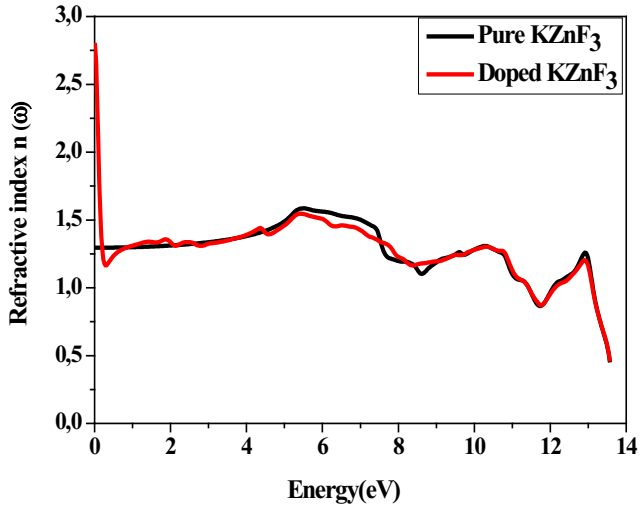

Figure 8: Refractive index as a function of energy of pure and doped $KZnF_3$.

The reflectivity R(ω), which describes the ability of a surface to reflect incident electromagnetic radiation, is analyzed from the results presented in Figure 9.

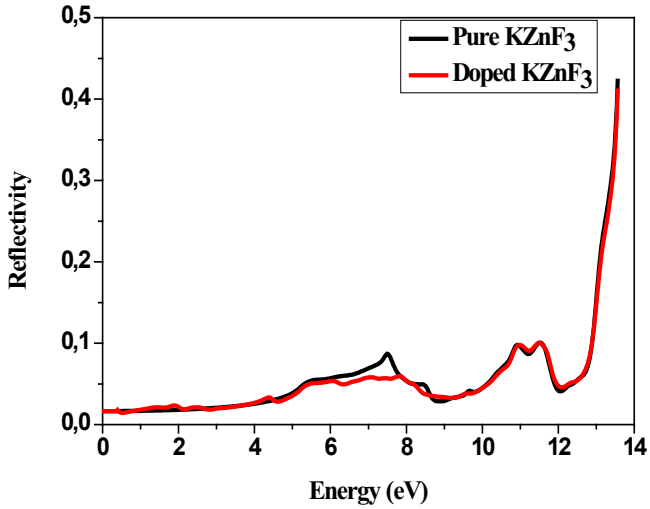

Figure 9: Reflectivity as a function of energy of pure and doped $KZnF_3$.

From the range of 0 to 4 eV, the reflectivity is lower, where this conduct is explained when comparing Figure 9 and the TDOS at the same range in Figure 4a, where no PDOS is observed. The results show that the reflectivity spectrum reaches its maximum values when the real ε1 (ω), shown in Figure 5a, becomes negative. This reflects a key property of metallic or semi-metallic materials, where negative values of ε1 (ω) mean total reflection of incident electromagnetic waves. This characteristic is essential for applications in optical devices such as selective mirrors

or optical filters. In addition, Cu doping modifies the position and intensity of reflectivity peaks, indicating a reorganization of $KZnF_3$'s electronic structure that optimizes its interactions with electromagnetic radiation. These adjustments enhance the material's potential for applications in advanced optical technologies, including the manufacture of anti-reflective coatings, high-performance mirrors and photovoltaic devices. Further analysis could also explore the effect of different levels of doping to refine optical properties and tailor the material to specific uses in a variety of fields.

4. CONCLUSION

This study combining analysis of the electronic, structural and optical properties of cubic perovskite $KZnF_3$, both in the pure and Cu-doped states, has demonstrated the notable impacts of doping on the fundamental characteristics of the material using the DFT, to address the electron–ion interaction. Density of states (DOS) analysis revealed that, in the pure state, electronic contributions are dominated by hybridized F-2p and K-4s orbitals. After Cu doping, Cu-3d impurity states emerged near the Fermi level, causing it to shift towards the VB, reflecting p-type semiconductor behavior. These modifications resulted in a 2.72 eV band gap decrease, facilitating a smooth electronic transition between the VB and CB. This hybridization between the F-2p, 3d-Zn and Cu-3d states, particularly pronounced in VB, also contributes to improved electronic and optical properties. In terms of optical properties, analysis of the dielectric functions ($\varepsilon_1(\omega)$ and $\varepsilon_2(\omega)$) revealed significant changes in the electronic response following doping. The real part, $\varepsilon_1(\omega)$, showed improved electronic polarization, while the imaginary part, $\varepsilon_2(\omega)$, revealed increased absorption in the visible spectrum. The absorption coefficient $\alpha(\omega)$ confirmed a better interaction with photons, essential for photovoltaic applications. In addition, the optical conductivity $\sigma(\omega)$ showed an increase in electron mobility, reinforcing the material's compatibility for optoelectronic devices. Refractive indices $n(\omega)$ and reflectivity $R(\omega)$ also showed optimized responses after doping, indicating increased potential for lightwave management in advanced technological applications. In summary, the simultaneous enhancement of the electronic and optical ($\varepsilon(\omega)$, $\alpha(\omega)$, $\sigma(\omega)$, $n(\omega)$, $R(\omega)$) properties of Cu-doped $KZnF_3$ demonstrates its potential for applications in photovoltaic devices, optical sensors and optoelectronic systems. These results illustrate the power of doping-based materials engineering to tailor perovskites to current and future technological needs.

Authors Contribution: Noureddine Elmeskini: Writing – original draft, visualization, validation, investigation, formal analysis, data curation, and conceptualization. Younes Ziat: Bibliography and references. Hamza Belkhanchi: Writing – original draft, and Ayoub Koufi: Visualization.

Funding: The authors are warmly grateful to the support of "The Moroccan Association of Sciences and Techniques for Sustainable Development (MASTSD), Beni Mellal, Morocco" and to its president, professor Charaf Laghlimi, for the valuable proposals.

Data Availability Statement: Not applicable.

Acknowledgments: A special thank you to Professor Hanane Reddad from Sultan Moulay Slimane University, Beni Mellal, Morocco, for her technical and scientific support, as well as her full collaboration and discussion during the different steps of the present investigation.

Conflicts of Interest: The authors declare that they have no conflict of interest.

REFERENCES

[1] G,Batra . Renewable energy economics: achieving harmony between environmental protection and economic goals. Social Science Chronicle, 2(2), 1-32 2023., https://doi.org/10.56106/

ssc.2023.009.

[2] L. P. S. S. Panagoda, R. A. H. T. Sandeepa, W. A. V. T. Perera,D. M. I. Sandunika, S. M. G. T. Siriwardhana, M. K. S. D. Alwis & S. H. S. Dilka. Advancements In Photovoltaic (Pv) Technology for Solar Energy Generation, Journal of Research Technology & Engineering, 4(30), 30-72. 2023.

[3] N. M. Manousakis,P. S. Karagiannopoulos,G. J. Tsekouras, & F. D. Kanellos. Integration of renewable energy and electric vehicles in power systems: a review. Processes, 11(5), 1544 2023., https://doi.org/10.3390/pr11051544.

[4] A. Koufi, Y. Ziat, H. Belkhanchi, & A. Bouzaid. DFT and BoltzTrap investigations on the thermal and structural characteristics of the perovskite MgCuH3 and MgCoH3. Computational Condensed Matter, e01010 2025., https://doi.org/10.1016/j.cocom.2025.e01010.

[5] Tu, Wenguang, Yong Zhou, and Zhigang Zou. "Photocatalytic conversion of CO2 into renewable hydrocarbon fuels: state-of-the-art accomplishment, challenges, and prospects." Advanced Materials 26.27 (2014): 4607-4626, https://doi.org/10.1002/adma.201400087.

[6] Chen, Xiaobo, et al. "Nanomaterials for renewable energy production and storage." Chemical Society Reviews 41.23 (2012): 7909-7937, https://doi.org/10.1039/C2CS35230C.

[7] Du, Shiwen, and Fuxiang Zhang. "General applications of density functional theory in photocatalysis." Chinese Journal of Catalysis 61 (2024): 1-36, https://doi.org/10.1016/S1872-2067(24)60006-9.

[8] M. H. Benkabou, M. Harmel, A. Haddou, A. Yakoubi, N. Baki, and R. Ahmed. "Structural , electronic , optical and thermodynamic investigations of NaXF3 (X = Ca and Sr): First-principles calculations.". Nanoscale, 56:131–144, 2018, https://doi.org/10.1016/j.cjph.2017.12.008.

[9] S. A. Shah, M. Husain, N. Rahman, M. Sohail, and R. Khan. "Insight into the struvtural, electronic, elastic, optical, and magnetic properties of cubic fluoroperovskites ABF3 (A = Tl , B = Nb , V) compounds: Probed by DFT.". Nanomaterials, 3, 2022, https://doi.org/10.3390/ma15165684.

[10] Z. Jin, Y. Wu, S. Li, Q. Wu, S. Chen, and Y. Chen. "Results in physics electronic structure , elastic , optical and thermodynamic properties of cubic perovskite NaBaF3 with pressure effects: First-principles calculations.". Results Phys., 22:103860, 2021, https://doi.org/10.1016/j.rinp.2021.103860.

[11] N. A.Bahmid, S. A. Siddiqui, H. D. Ariyanto, K. S.Sasmitaloka, N. B.Rathod,S. K. Wahono, ... & A. W. Indrianingsih,Cellulose-based coating for tropical fruits: method, characteristic and functionality. Food Reviews International, 40(4), 1069-1092. 2024. https://doi.org/10.1080/87559129.2023.2209800.

[12] S.Wang,Y. Wan,N. Song, Y. Liu, T. Xie, & B.Hoex.Automatically Generated Datasets: Present and Potential Self-Cleaning Coating Materials. Scientific Data, 11(1), 146 2024., https://doi.org/10.1038/s41597-024-02983-0.

[13] A. A. Pasha, H. Khan, M. Sohail, N. Rahman, R. Khan, and A. Ullah. "A computational first principle examination of the elastic, optical, structural and electronic properties of AlRF3 (R = N, P) fluoroperovskites compounds.". Molecules, 28, 2023, https://doi.org/10.3390/molecules28093876.

[14] A. Koufi, Y. Ziat, H. Belkhanchi, ... and F. Z. Baghli. A computational study of the structural and thermal conduct of MgCrH3 and MgFeH3 perovskite-type hydrides: FP-LAPW and BoltzTraP insight. E3S Web of Conferences (Vol., 582, p. 02003). 2024. EDP Sciences. https://doi.org/10.1051/e3sconf/202458202003.

[15] R. Ullah and A. H. Reshak. "Pressure-dependent elasto-mechanical stability and thermoelectric properties of MYbF3 (M = Rb , Cs) materials for renewable energy.". International

Journal of Energy Research, 45:1–13, 2021, https://doi.org/10.1002/er.6408.

[16] W. Ullah, R. Nasir, M. Husain, N. Rahman, and H. Ullah. "Revealing the remarkable structural, electronic, elastic, and optical properties of Zn-based fluoropervskite ZnXF3 (x = Sr, Ba) employing DFT. ". Indian J. Phys., 3, 2024, https://doi.org/10.1007/s12648-024-03146-y.

[17] N. Chouit, S. A. Korba, M. Slimani, H. Meradji, S. Ghemid, and R. Khenata. "First-principles study of the structural, electronic and thermal properties of CaLiF3. ". Phys. Scr., 88:139–153, 2013, 10.1088/0031-8949/88/03/035702.

[18] J. Zhang, Y. Chen, S. Chen, J. Hou, R. Song, and Z. F. Shi. "Electronic structure, mechanical, optical and thermodynamic properties of cubic perovskite InBeF3 with pressure effects: First-principles calculations.". Results Phys., 50:106590, 2023, https://doi.org/10.1016/j.rinp.2023.106590.

[19] M. R. Kabli, J. ur Rehman, M. Bilal Tahir, M. Usman, A. Mahmood Ali, and K. Shahzad. "Structural, electronics and optical properties of sodium based fluoroperovskites NaXF3 (X = Ca, Mg, Sr and Zn): First principles calculations.", Phys. Lett. Sect. A Gen. At. Solid State Phys., 412:127574, 2021. https://doi.org/10.1016/j.physleta.2021.127574.

[20] M. I.Abdulraheem, H., Li, L. Chen, A. Y. Moshood, W. Zhang, Y.Xiong, ... & Hu, J. Recent Advances in Dielectric Properties-Based Soil Water Content Measurements. Remote Sensing, 16(8), 1328. 2024., https://doi.org/10.3390/rs16081328.

[21] J. ur Rehman, M. Usman, M. B. Tahir, and A. Hussain. "First-principles calculations to investigate structural , electronic and optical properties of Na based fluoroperovskites NaXF3 (X = Sr, Zn). ". Solid State Commun., 334–335:114396, 2021., https://doi.org/10.1016/j.ssc.2021.114396.

[22] T. N. Ishimatsu, N. T. Erakubo, H. M. Izuseki, Y. K. Awazoe, and D. A. P. Awlak. "Band structures of perovskite-like fluorides for vacuumultraviolet-transparent lens materials.". Japanese Journal of Applied Physics, 41:10–13, 2002., DOI 10.1143/JJAP.41.L365.

[23] A.Jehan, M. Husain, N. Rahman,V. Tirth, N. Sfina,M. Elhadi, ... & S. N.Khan, Investigating the structural, elastic, and optoelectronic properties of LiXF3 (X= Cd, Hg) using the DFT approach for high-energy applications. Optical and, Quantum Electronics. 56(2) 169. 2024. https://doi.org/10.1007/s11082-023-05750-4.

[24] M. Usman, J. ur Rehman, and M. B. Tahir. "Screening of ABF3 fluoroperovskites by using first-principles calculations.". Solid State Commun., 369:1–6, 2023, https://doi.org/10.1016/j.ssc.2023.115198.

[25] H. M.Ghazi, & A. H. Reshak. First principle investigation of the structural, electronic, optical, and elastic properties of Ba-based fluoroperovskite (BaYF3; Y= Li, Na, K, and Rb) compounds. Journal of Theoretical and Applied Physic, 2024., 18(5), 1-13. 10.57647/j.jtap.2024.1805.58.

[26] D.Ceriotti, P. Marziani, F. M.Scesa, A.Collorà, C. L. Bianchi, L. Magagnin, & M.Sansotera. Mechanochemical synthesis of fluorinated perovskites KCuF 3 and KNiF 3. RSC Mechanochemistry, 1(5), 520-530. 2024., https://doi.org/10.1039/d4mr00037d.

[27] D. A.Ahmed, S.Bağcı, E.Karaca, & H. M.Tütüncü. Elastic properties of ABF3 (A: Ag, K and B: Mg, Zn) perovskites. In AIP Conference Proceedings (Vol. 2042, No. 1). AIP Publishing 2018., https://doi.org/10.1063/1.5078907.

[28] L.L.Boyer, P.J.Edwardson, Perovskite to antiperovskite in abf3 compounds. Ferroelectrics 104, 417–422 1990,, https://doi.org/10.1080/00150199008223849.

[29] M. Miri , Y. Ziat, H. Belkhanchi, A. Koufi, Y. A. El Kadi, Modulation des propriétés électroniques et optiques de la pérovskite InGeF3 sous pression : une approche computationnelle,

"The European Physical Journal B", 2025. https://link.springer.com/journal/10051

[30] M.Mubashir, Z. Bibi, M.Ali, M. Muzamil, U.Afzal, & M. D.Albaqami, First-principles prediction of antimony based XSbF3 (X= Be, Mg, Ca and Sr) fluoroperovskites: An insight into structural, optoelectronic and thermal properties. 2024., Physica B: Condensed Matter, 685, 415986. https://doi.org/10.1016/j.physb.2024.415986.

[31] S.u Zaman, I.Ghani, J.Riaz, A.Bibi, & M.Arif, DFT-based ab initio study of structural, electronic, optical and thermodynamics properties of Al based fluoroperovskite AlMF3 (M= Ca and Cd). Optical and Quantum Electronics, 56(7), 1205. 2024., https://doi.org/10.1007/s11082-024-07130-y.

[32] J.Khan, & M.Faisal, Exploring the Potential of Nitrogen-Based Anti-Perovskite Compounds for Solar Cells: A Theoretical Investigation of Their Structural and Optoelectronic Properties Using Density Functional Theory (Dft)., http://dx.doi.org/10.2139/ssrn.4888926.

[33] N.Rahman ; M.Husain; J.Yang; M. Sajjad ; G.Murtaza ; M.Ul Haq ; A.Habib ; Zulfiqar; A. Rauf ; A.Karim ; et al. First principle study of structural, electronic, optical and mechanical properties of cubic fluoro-perovskites: (CdXF3, X = Y, Bi)., Eur. Phys. J. Plus 136, 347. 2021. https://doi.org/10.1140/epjp/s13360-021-01177-6.

[34] L.Tian ; Z.Hu ; X.Liu ; Z. Liu ; P.Guo ; B.Xu ; Q.Xue ; H.-L.Yip ; F.Huang ; Y.Cao, Fluoro- and amino-functionalized conjugated polymers as electron transport materials for perovskite solar cells with improved efficiency and stability., ACS Appl. Mater. Interfaces 11, 5289–5297. 10.1021/acsami.8b19036 2019,.

[35] Turner, G. Global Renewable Energy Market Outlook 2013. Bloom. New Energy Financ. 2013, 26, 506. 7. Mahmoud, N.T.; Khalifeh, J.M.; Mousa, A.A. Effects of rare earth element Eu on structural, electronic, magnetic, and optical properties of fluoroperovskite, compounds SrLiF3: First principles calculations. Phys. B Condens. Matter 2019, 564, 37–44. https://doi.org/10.3390/ma15165684.

[36] M. Miri, Y. Ziat, H. Belkhanchi, and YA. El Kadi, The effect of pressure on the structural, optoelectronic and mechanical conduct of the XZnF3(X = Na, K and Rb) perovskite: First-principles study,, "International Journal of Modern Physics B", 2024, 2550096. https://doi.org/10.1142/S0217979225500961.

[37] X. Wang, W. Li, H. Zhao, S. Wang ... & P. Wang. Yb3+-Yb3+ cooperative upconversion in oxyfluoride glass and glass ceramics. Journal of Luminescence, 226, 117461. 2020., https://doi.org/10.1016/j.jlumin.2020.117461.

[38] A.Meziani , D.Heciri , & H. Belkhir. Structural, electronic, elastic and optical properties of fluoro-perovskite $KZnF_3$*. Physica B: Condensed Matter, 406(19), 3646-3652 2011., https://doi.org/10.1016/j.physb.2011.06.063.*

[39] N.Erum , & M. A.Iqbal. Ab initio study of structural, opto-electronic, elastic, and thermal properties of $KZnF_3$*. Canadian Journal of Physics, 99(7), 551-558 2021., https://doi.org/10.1139/cjp-2020-0303.*

[40] A.Ayub , H. M. N.Ullah , M.Rizwan , A. A.Zafar, Z.Usman , & U.Hira. Impact of Zn alloying on structural, mechanical anisotropy, acoustic speeds, electronic, optical, and photocatalytic response of KMgF3 perovskite material., Materials Science in Semiconductor Processing, 173, 108049. 2024. https://doi.org/10.1016/j.mssp.2023.108049.

[41] A. Mubarak, and S. Al-Omari,First-principles calculations of two cubic fluoropervskite compounds: RbFeF3 and RbNiF3., J. Magn. Magn. Mater. 2015, 382, 211–218. https://doi.

org/10.1016/j.jmmm.2015.01.073.

[42] M.Miri , Y.Ziat , H.Belkhanchi , Z.Zarhri , & Y. A.El Kadi. Structural and optoelectronic properties of LiYP (Y= Ca, Mg, and Zn) half-Heusler alloy under pressure: A DFT study. Physica B: Condensed Matter, 667, 415216 2023., https://doi.org/10.1016/j.physb.2023.415216.

[43] M.Miri ,Y. Ziat , H.Belkhanchi , & Y. A. El Kadi. Structural, elastic, and opto-electronic conduct of half Heusler Li (Ca, Mg, Zn) N alloys: Ab initio computation. Solid State Communications, 396, 115765 2025., https://doi.org/10.1016/j.ssc.2024.115765.

[44] Ziat, Y., Belkhanchi, H., & Zarhri, Z. (2025). DFT analysis of structural, electrical, and optical properties of S, Si, and F-Doped GeO2 Rutile: implications for UV-transparent conductors and photodetection. Solar Energy and Sustainable Development, 14(1), 74-89. https://doi.org/10.51646/jsesd.v14i1.232.

[45] Y.Ziat , H.Belkhanchi , Z.Zarhri , & S.Rzaoudi. Electronegativity effect of (Z=S, O, F and Cl) doping on the electrical, electron density and optoelectronic properties of half-Heusler LiMgP: DFT overview. Physica B: Condensed Matter, 646,, 414324. 2022. https://doi.org/10.1016/j.physb.2022.414324.

[46] P. Blaha, K. Schwarz, F. Tran, R. Laskowski, G.K. Madsen, & L. D. Marks. WIEN2k: An APW+ lo program for calculating the properties of solids. The Journal of chemical physics, 152(7). 2020, https://doi.org/10.1063/1.5143061.

[47] J. P.Perdew , K.Burke , & M.Ernzerhof. Generalized gradient approximation made simple. Physical review letters, 77(18), 3865.1996., https://doi.org/10.1103/PhysRevLett.77.3865.

[48] T. Seddik, & al. "Elastic, electronic and thermodynamic properties of fluoro-perovskite $KZnF_3$ *via first-principles calculations." Applied Physics A 106 2012: 645-653., https://doi.org/10.1007/s00339-011-6643-2.*

[49] K.Knox. Perovskite-like fluorides. I. Structures of KMnF3, KFeF3, KNiF3 and $KZnF_3$*. Crystal field effects in the series and in KCrF3 and KCuF3. Acta Crystallographica, 14(6), 583-585. 1961., https://doi.org/10.1107/S0365110X61001868.*

[50] Y Ziat, Z Zarhri, H Belkhanchi, O Ifguis, A D Cano, & C Lazrak . Effect of Be and P doping on the electron density, electrical and optoelectronic conduct of half-Heusler LiMgN within ab initio scheme. Physica Scripta, 97(10): 105802 2022;, 10.1088/1402-4896/ac8b40.

[51] A. Bouzaid, Y. Ziat, H. Belkhanchi, H, Hamdani, A. Koufi, M. Miri, ... & Z. Zarhri. Ab initio study of the structural, electronic, and optical properties of MgTiO3 perovskite materials doped with N and P. E3S Web of Conferences, (Vol. 582, p. 02006). EDP Sciences 2024. https://doi.org/10.1051/e3sconf/202458202006.

[52] Y. Ziat, Z. Zarhri, M. Hammi, H. Belkhanchi, & A. C. Bastos. Effect of (Na, Si, Al, K or Ca) doping on the electronic structure and optoelectronic properties of half-Heusler LiMgN alloy: Ab initio framework., Solid State Communications, 343, 114665, 2022. https://doi.org/10.1016/j.ssc.2022.114665.

[53] R Majumder, M M Hossain, & D Shen . First-principles study of structural, electronic, elastic, thermodynamic and optical properties of LuPdBi half-Heusler compound. Modern Physics Letters B, 33(30):1950378 2019;, https://doi.org/10.1142/S0217984919503780.

[54] A. Bouzaid, Y. Ziat, & H. Belkhanchi. Prediction the effect of (S, Se, Te) doped MgTiO3 on optoelectronic, catalytic, and pH conduct as promised candidate photovoltaic device: Ab initio framework., International Journal of Hydrogen Energy, 100, 20-32. 2025. https://doi.org/10.1016/j.ijhydene.2024.12.284.

[55] C. M. I.Okoye, "Theoretical study of the electronic structure, chemical bonding and optical properties of KNbO3 in the paraelectric cubic phase." Journal of Physics: Condensed Matter 15.35 : 5945 2003, 10.1088/0953-8984/15/35/304 .

[56] S Saha, T P Sinha, & A Mookerjee . Electronic structure, chemical bonding, and optical properties of paraelectric BaTiO 3. Physical Review B, 62(13): 8828 2000;, https://doi.org/10.1103/PhysRevB.62.8828.

[57] Delin, Anna, et al. "Optical properties of the group-IVB refractory metal compounds." Physical Review B 54.3 (1996): 1673, https://doi.org/10.1103/PhysRevB.54.1673.

[58] Y.Ziat, A.Abbassi, A.Slassi , M.Hammi , A. A. Raiss , O. E.Rhazouani , ... & A. E. Kenz. First-principles investigation of the electronic and optical properties of Al-doped FeS 2 pyrite for photovoltaic applications., Optical and Quantum Electronics, 48, 1-8. 2016. https://doi.org/10.1007/s11082-016-0781-x.

[59] M. Rizwan, A. Ayub, M. Shakil, Z. Usman, S. S. A. Gillani, H. B. Jin, & C. B. Cao. Putting DFT to trial: For the exploration to correlate structural, electronic and optical properties of M-doped (M= Group I, II, III, XII, XVI), lead free high piezoelectric c-BiAlO3. Materials Science and Engineering: B, 264, 114959 2021. https://doi.org/10.1016/j.mseb.2020.114959.

[60] Ilyas, Asif, & al. "Investigation of the structural, electronic, magnetic, and optical properties of $CsXO_3$ (X= Ge, Sn, Pb) perovskites: A first-principles calculations." Optik 244 : 167536 2021, https://doi.org/10.1016/j.ijleo.2021.167536.